The International Journal of Advanced Manufacturing Technology (2020) 109:2393–2407
https://doi.org/10.1007/s00170-020-05789-7

ORIGINAL ARTICLE

Identification of milling chatter based on a novel frequency-domain search algorithm

Liu Chang [1,2] · Xu Weiwei [1,2] · Gao Lei [1,2]

Received: 31 January 2020 / Accepted: 17 July 2020 / Published online: 31 July 2020

Abstract

Chatter is a kind of self-excited vibration, which will result in very poor quality and dimensional accuracy on the machined surface, even a harmful effect on machining operation. A simple, reliable, and accurate chatter identification algorithm is crucial for taking control strategy before it is fully developed. This paper proposes a novel frequency-domain search (FDS) algorithm to identify the chatter during milling. An identification feature based on vibration base frequency is extracted according to the FDS algorithm, where the complicated signal processing algorithms are not needed before feature extraction. Compared with most of the existing identification features, the introduced feature does not need to set thresholds according to different machining conditions. Meanwhile, the feature extraction only needs a small amount of data to guarantee the timeliness of identification. Hammer test and milling experiments with various cutting parameters are carried out, and both force signal and vibration signal in the experiments are utilized to validate the effectiveness of the proposed algorithm. The results show that the proposed algorithm can identify the milling chatter accurately, whether using force signal or vibration signal, even slight chatter in the initial machining stage can be identified. Furthermore, the research reveals that dominant chatter frequencies appear around the natural frequency of the spindle-tool system but do not exactly equal to its natural frequency. The chatter frequencies are found to be determined by the combination of natural characteristics of the system and cutting conditions.

Keywords Chatter identification · Vibration base frequency · Frequency-domain search · Chatter frequencies · Natural frequency

Nomenclature

a_e	Radial depth of cut (mm)
a_p	Axial depth of cut (mm)
f_C	Vibration base frequency (Hz)
f_{cfr}	Searching range of the proposed algorithm
f_{cfr}^a	Left interval of the searching range (Hz)
f_{cfr}^b	Right interval of the searching range (Hz)
f_d	Difference between f_{IMF} and f_{TPF} (Hz)
f_{IMF}	Identified maximum frequency (Hz)
f_{MCF}	Multiple chatter frequencies (Hz)
f_{SRF}	Spindle rotation frequency (Hz)
f_{STF}	Surface topography frequency (Hz)
f_{TPF}	Tooth pass frequency (Hz)
f_z	Feed per tooth (Hz)
F_x, F_y	Cutting force signal in x and y directions, respectively (N)
k_b	Multiple of initial search frequency
L_w	Measured length of surface profile (mm)
n	Spindle speed (rpm)
n_w	Number of the corrugations in the scope of L_w
N_t	Number of teeth
S_x, S_y	Spectrum of cutting force signal of x and y directions, respectively

✉ Liu Chang
liuchang@tiangong.edu.cn

[1] Tianjin Key Laboratory of Advanced Mechatronics Equipment Technology, Tiangong University, Tianjin 300387, China

[2] School of Mechanical Engineering, Tiangong University, Tianjin 300387, China

1 Introduction

Milling is a commonly used machining method to achieve the complex surface and precision parts, as well as the productivity improvement and cost-effectiveness in aviation and electronic industry. However, the inappropriate cutting parameters and experimental conditions will result in chatter vibration, and correspondingly leads to very poor surface quality and dimensional accuracy on the machined workpiece [1, 2].

Meanwhile, to prevent a harmful effect on machining operation, the unavoidable and unscheduled downtime will be performed, which not only in terms of time lost but also in terms of tool damage [3, 4].

Chatter belongs to a kind of self-excited vibration during the machining, which occurs at specific combinations of cutting parameters, such as axial depth of cut and spindle speed. As well known, the analytical modeling methods are usually utilized to build a stability lobe diagram (SLD) [5, 6]. Further, the appropriate axial depth of cut and spindle speed will be selected based on the SLD to avoid the occurrence of milling chatter. However, the predicted models with inevitable simplifications cannot describe the complex milling system accurately and prevent the occurrence of chatter completely [7, 8]. The online and timely identification for milling chatter has been an essential strategy to improve the machined quality and machining productivity. It has been estimated that timely identification of tool condition and machining process could effectively reduce the unnecessary downtime with a saving of 10–40% [9, 10].

The current researches have developed efficient monitoring systems to identify the chatter by using sensor information, such as dynamic force [11, 12], acceleration [13, 14], acoustic signal [15], etc., and correspondingly maintain the machining process in stable conditions. Once the machining signals are collected, the crucial task for chatter identification is to extract appropriate indicators to distinguish the chatter and stable conditions. Note that the extracted indicators should contain the chatter-related information so that the chatter can be identified accurately. However, as well known that the machining signals containing the relevant and irrelevant chatter information are nonlinear and nonstationary, signal processing methods are thus commonly carried out before feature extraction to improve the accuracy of chatter identification. Table 1 summarizes some recent researches on the identification of milling chatter.

The above indicators are suitable for chatter identification under the given conditions. It is found that a threshold is commonly set artificially or based on an auxiliary algorithm according to different machining conditions to identify the chatter and stable condition. That is to say, the threshold should be redetermined in a new machining environment. Furthermore, the auxiliary and more complicated signal processing algorithms are performed to further improve the accuracy and robustness of the chatter identification. However, these auxiliary algorithms on threshold setting and signal processing will reduce the applicability and the timeliness of the identification algorithms in semiautomatic and fully automatic manufacturing environments. In industry, a simple identification algorithm is highly desirable where the indicators can be performed easily without time-consuming recalibration processes to achieve the timely identification of milling chatter [26].

In order to avoid full deterioration of the workpiece surface quality, some researches were proposed to achieve chatter identification in the early stage of chatter outbreak so that the chatter suppression strategy can be timely performed. Cao et al. [19] calculated the minimum quantization error (MOE) of a SOM neural network and multiple feature vectors as an indicator. Correspondingly, 3σ criterion is proposed to set the threshold of MOE to identify chatter before the workpiece surface is fully deteriorated. Wang et al. [27] found that the first intrinsic mode functions (IMF) of Hilbert-Huang spectrum of the measured cutting force are sensitive to the early stage of chatter outbreak. Zhang et al. [28] decomposed the cutting force signals into sub-signals by using VMD and wavelet packet decomposition (WPD). Then the energy

Table 1 Summary of the milling chatter identification

Signal processing algorithms	Identification indicators	Determination of threshold	Ref.
–	Coefficient of variation of RMS sequence	Milling experiments	[16]
EEMD	Fractal dimension and power spectral entropy	Milling experiments	[17]
HHT	Normalized energy ratio and coefficient of variation	Gaussian mixture algorithm	[18]
SOM neural network	Euclidean distance between the best matching unit of SOM neural network and the feature vectors	3σ criterion	[19]
VMD	Multiscale permutation entropy and multiscale power spectral entropy	Laplacian score based feature selection	[20]
WPT	Time-domain and frequency-domain features	Feature weights based on SVM-RFE	[21]
WPT and HHT	Mean value and standard deviation of the Hilbert-Huang spectrum	Milling experiments	[22]
A wavelet-based maximum likelihood estimation algorithm	Spectral parameter related to the measured power spectra	Milling experiments	[23]
Time-frequency analysis	Energy ratio based on the Wigner time-frequency distribution	Milling experiments	[24]
Kalman filter and Teager-Kaiser nonlinear energy operator	Energy ratio of chatter component to the total vibration	Milling experiments	[25]

WPT, wavelet packet transform; *HHT*, Hilbert-Huang transform; *VMD*, variational mode decomposition; *EEMD*, ensemble empirical mode decomposition; *SOM*, self-organizing map; *SVM-RFE*, support vector machine recursive feature elimination

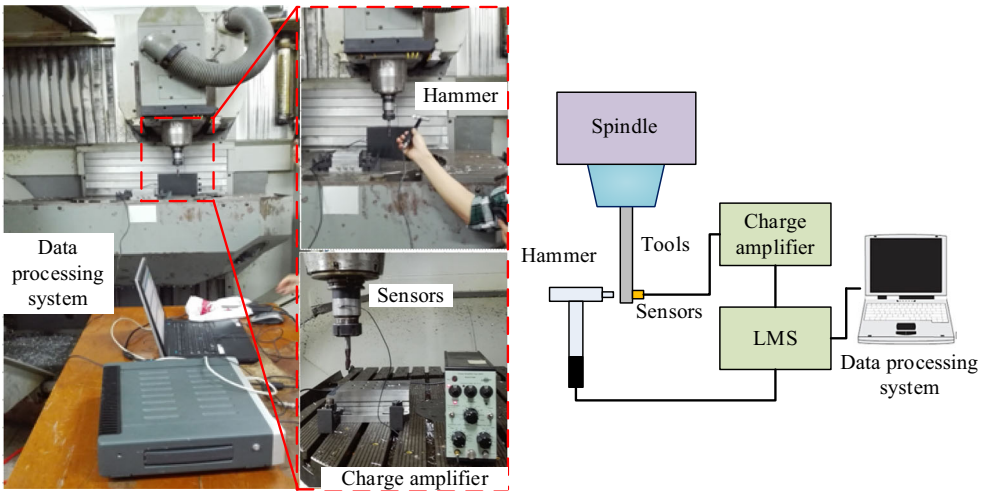

Fig. 1 Hammer test. **a** Experimental setup. **b** Schematic diagram

entropy is extracted from the sub-signals to identify chatter at the early stage. Yang et al. [1] proposed an optimized variational mode decomposition (OVMD) to decompose cutting force signal and extracted entropy features by using a simulated annealing (SA) algorithm. The onset of chatter is detected based on the relative changes of the entropy.

Another issue in chatter identification is to estimate dominant chatter frequencies in order to provide important information for chatter suppression. However, most of the time series analysis methods [29–32] cannot recognize the chatter frequencies, especially the dominant chatter frequencies [33]. Dijk et al. [34] constructed a transfer function model and solved the dominant root as the dominant chatter frequencies. However, the accuracy of identification results is greatly limited by the accuracy of the constructed model. Wan et al. [35] utilized a time-frequency method based on EEMD and HHT to extract the dominant chatter frequencies.

As described above, a simple identification algorithm based on the indicator without setting threshold is more appropriate to the industrial conditions. Meanwhile, the methods should solve two issues, the timely chatter identification and the identification of dominant chatter frequencies. It is known that a new periodic motion accompanied by a vibration base frequency will superimpose in milling motion during the chatter, even the slight chatter occurs [36, 37]. Correspondingly, the vibration base frequency superimposes to the tooth pass frequencies to form the chatter frequencies. This paper tries to introduce the vibration base frequency as an indicator and perform a simple frequency-domain search algorithm to achieve the identification of milling chatter and the chatter frequencies.

The remainder of the paper is organized as follows. Section 2 describes the hammer test and the selection of cutting parameters for chatter identification. An identification algorithm based on frequency-domain search (FDS) is given in Section. 3. To improve the efficiency and robustness of the FDS algorithm, the machining signal in the appropriate direction and the main frequency range of chatter are determined. Section 4 validates the accuracy of the proposed algorithm and analyzes the effectiveness of the proposed algorithm when using cutting force signal, vibration signal, and a small amount of signal data. Section 5 discusses the spectral characteristics of the chatter signal and the relationship among the natural frequency of the spindle-tool system, cutting parameters, and chatter frequencies. Some conclusions are given in Section. 6.

Table 2 The cutting tool information

Type of tool	Number of flutes	Stick out (mm)	Diameter (mm)
Tungsten steel end mill	2	60	6

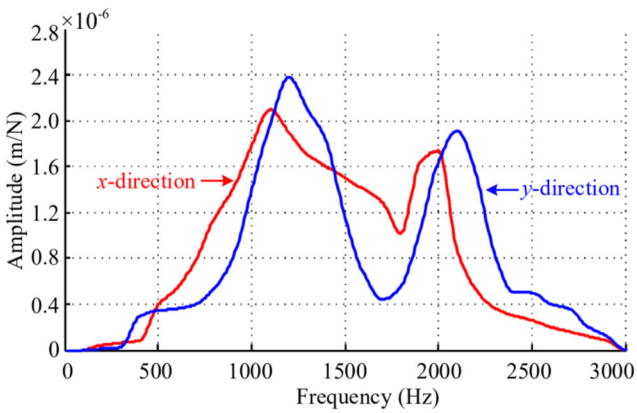

Fig. 2 Measured FRF of the spindle-tool system

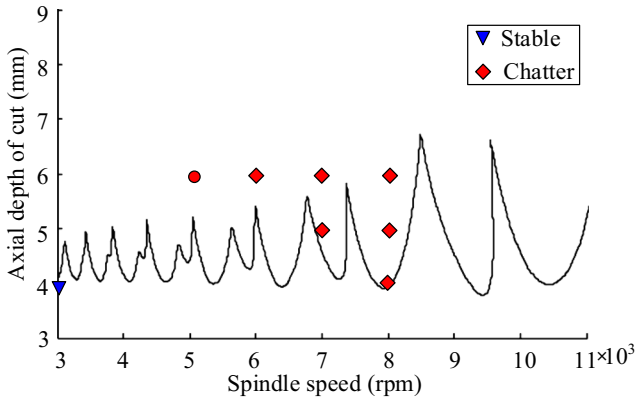

Fig. 3 Experiment result analysis for chatter stability prediction

2 Experiments

2.1 Hammer test and determination of the SLD

The SLD is commonly constructed to define the stable and chatter condition. The cutting parameters (spindle speed and axial depth of cut) in stable and chatter machining can be correspondingly selected. To determine the SLD and correspondingly analyze the characteristic of chatter frequency, hammer tests were carried out to obtain the natural characteristics of the spindle-tool system. Figure 1a, b shows the experimental setup and schematic diagram of the hammer tests, respectively. The hammer (type: MSC-1) knocked on the cutting tool to produce impulse response. Correspondingly, two acceleration sensors were absorbed on the cutting tool to obtain the vibration response in x and y directions, respectively. Note that the x and y directions are just orthogonal, which do not have a specific definition of direction. A charge amplifier (type: DLF-3) was connected with a 16-channel data processing system (type: AD8304) to achieve the data acquisition, amplification, and A/D transformation. The detailed information of the used cutting tool is given in Table 2, where a two-flute tungsten steel end mill with a stick out of 60 mm and a diameter of 6 mm is used. The type of tool holder used in the experiment is SK40-ER20-100. Figure 2 shows the measured frequency response function (FRF) of the spindle-tool system in x and y directions.

The cutting force coefficients and the transfer function of the spindle-tool system are necessary to build an SLD. The identification algorithm for cutting force coefficients can be found in ref. [38]. The transfer function of the spindle-tool system is measured based on the hammer tests (Fig. 1), and the prediction algorithm of the SLD can be found in ref. [39]. The width of cut is 0.5 mm, and the material used is Al7075-T6 aviation aluminum. Figure 3 shows the predicted SLD and the selected cutting condition in this paper. The blue inverted triangle and the red rhombus represent the normal and chatter conditions, respectively.

2.2 Milling experiments

Table 3 gives the cutting parameters for milling chatter identification where down milling experiments were performed. The feed per tooth f_z and radial depth of cut a_e are fixed as 0.15 mm/tooth and 0.5 mm, respectively. The axial depth of cut a_p and spindle speed n are determined according to Fig. 3. The first test belongs to stable machining, and the other five tests belong to chatter machining. As shown in Fig. 4, milling experiments were carried out on DMU80T multi-axis vertical machining center based on the selected cutting parameters. A dynamometer (type: Kister 9257A) was connected to a charge amplifier (type: Kistler 5070) and mounted on the workbench to measure the dynamic cutting force signal. The sampling frequency was 10 kHz. The workpiece is Al7075-T6 aviation aluminum, and the cutting tool is a tungsten steel end mill with two teeth. The x and z directions are parallel to the feed direction and tool axis direction. The y direction is perpendicular to the feed direction.

3 Algorithm

3.1 Feature analysis and extraction

Generally, the spectrum of milling signals comprises different kinds of frequency components, such as spindle rotation frequency (f_{SRF}) and its frequency multiplication, tooth pass

Table 3 The selected cutting parameters for chatter identification

Test	Milling type	Feed per tooth f_z (mm/tooth)	Radial depth of cut a_e (mm)	Axial depth of cut a_p (mm)	Spindle speed n (rpm)	Milling condition
1	Down milling	0.15	0.5	4	3000	Stable
2	Down milling	0.15	0.5	4	8000	Chatter
3	Down milling	0.15	0.5	5	7000	Chatter
4	Down milling	0.15	0.5	5	8000	Chatter
5	Down milling	0.15	0.5	6	6000	Chatter
6	Down milling	0.15	0.5	6	7000	Chatter
7	Down milling	0.15	0.5	6	8000	Chatter

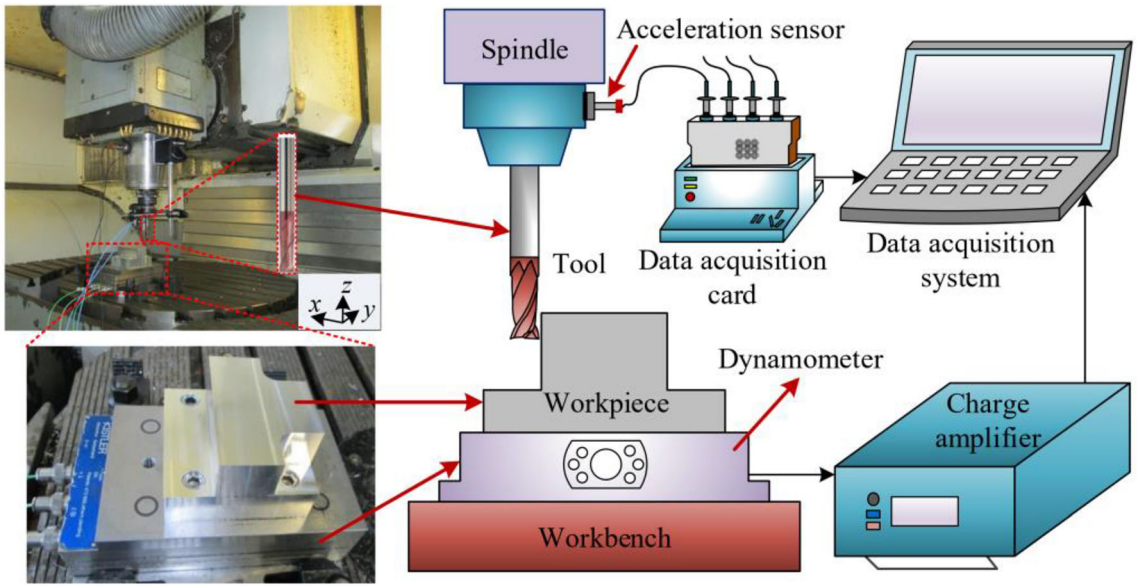

Fig. 4 Milling experiment setup

frequency (f_{TPF}) and its frequency multiplication, chatter frequencies, and natural frequencies of the system. In the following section, the frequency multiplication of f_{SRF} and frequency multiplication of f_{TPF} are all named as f_{SRF} and f_{TPF}, respectively. Note that the chatter spectrum is not a single frequency, but has multi-order properties. That is to say, multi chatter frequencies exist among the spectrum of milling signals. The calculations of f_{SRF} and f_{TPF} are given as shown in Eqs. (1) and (2), respectively.

$$f_{SRF} = \left\{ m\frac{n}{60} \right\} (\text{Hz}),\ m = 1,\ 2, \cdots \tag{1}$$

$$f_{TPF} = \left\{ m\frac{N_t \cdot n}{60} \right\} (\text{Hz}),\ m = 1,\ 2, \cdots \tag{2}$$

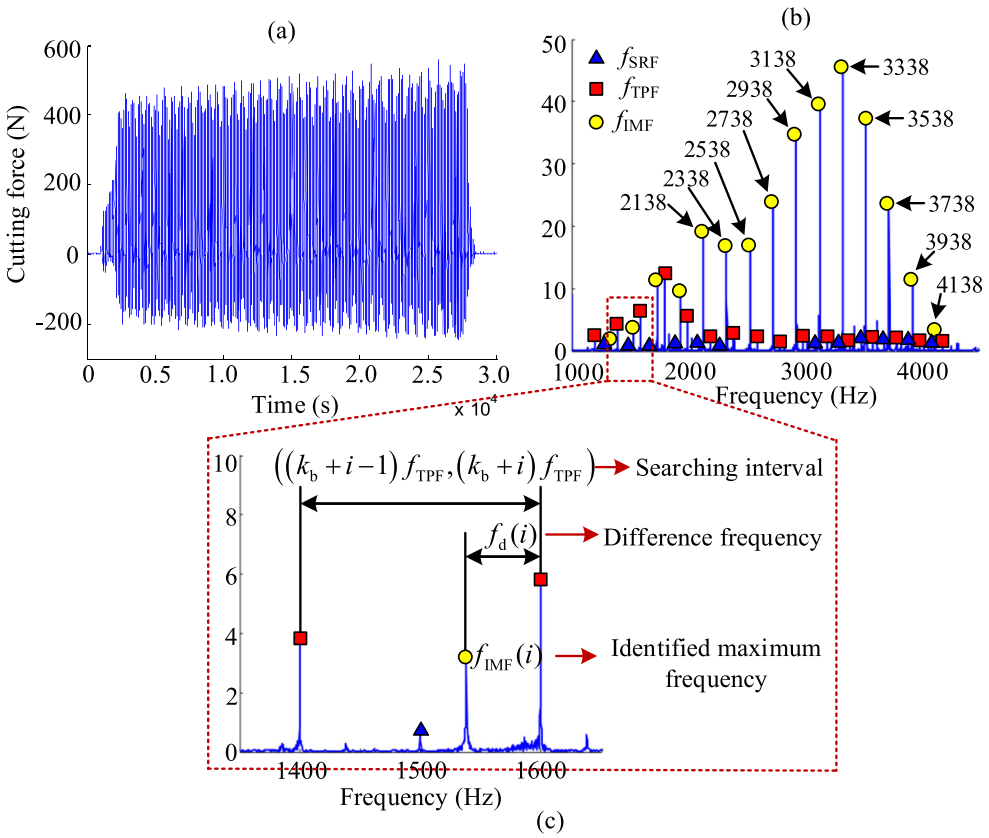

Fig. 5 Schematic diagram of the FDS algorithm. **a** The chatter cutting force signals. **b** Spectral analysis of the chatter cutting force signals. **c** Schematic diagram of the proposed FDS algorithm (A down-milling experiment is performed, where f_z is 0.15 mm/tooth, a_e is 0.5 mm, a_p is 8 mm, and n is 6000 rpm)

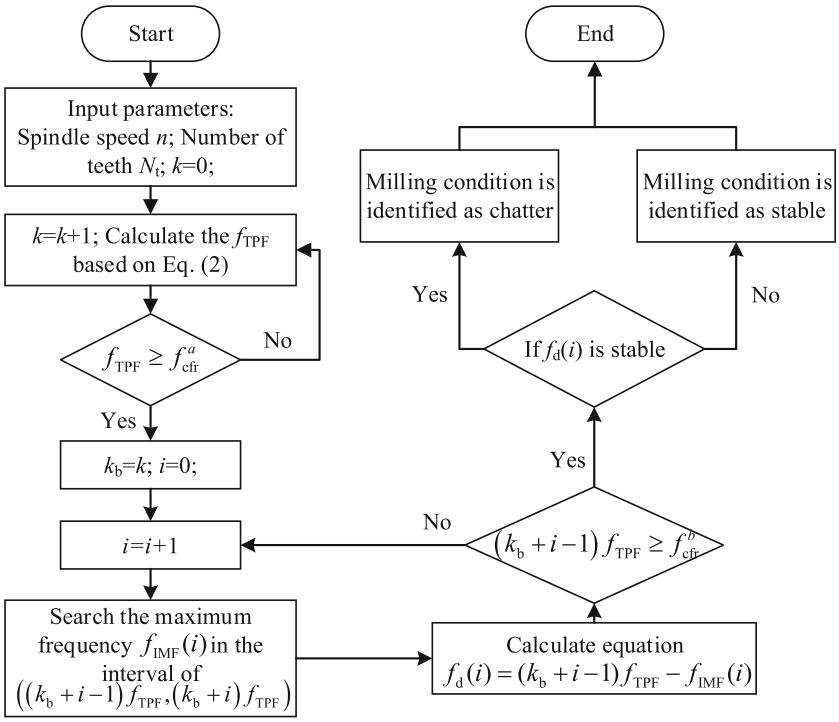

Fig. 6 Flowchart of the chatter identification based on the FDS algorithm

where N_t is the number of the tool tooth.

An important characteristic of the chatter is that a new periodic motion accompanied by a base frequency will appear and correspondingly superimpose in milling motion. Here, the base frequency is named as vibration base frequency (f_C). The appearance of the base frequency means the instability of

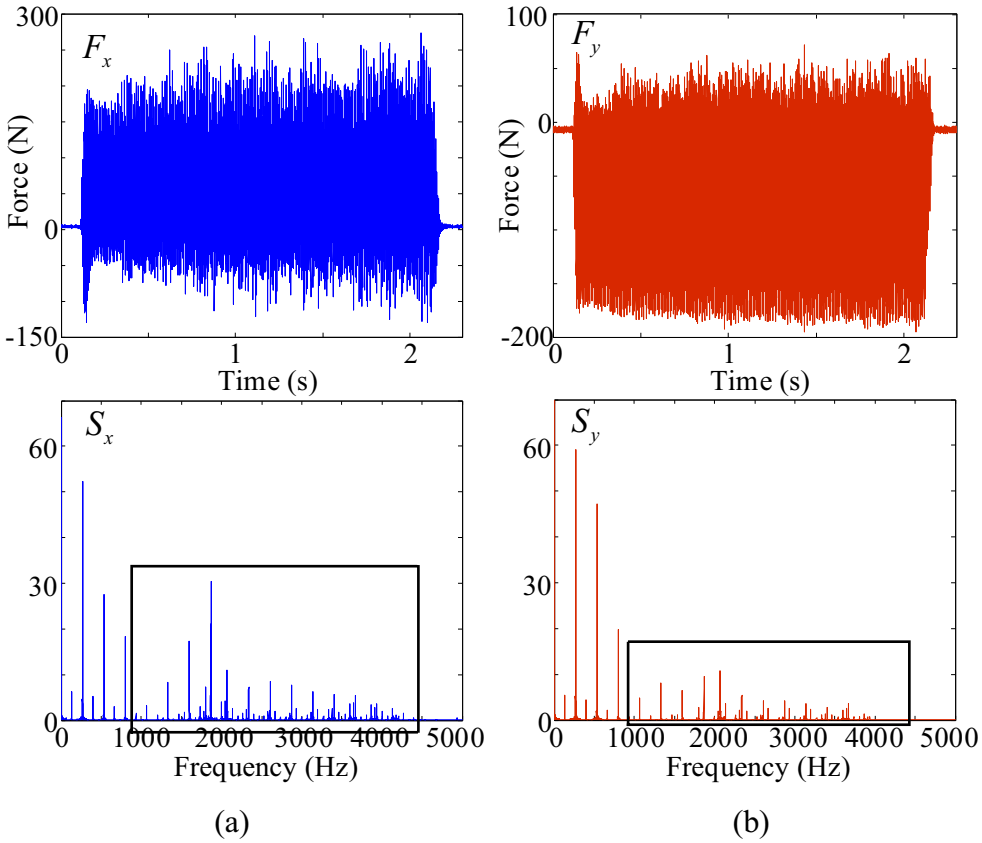

Fig. 7 Cutting force signal and its spectrum of test 7: **a** x direction and b y direction (the spindle speed is 8000 rpm, the axial depth of cut is 6 mm, the radial depth of cut is 0.5 mm, and feed per tooth is 0.15 mm)

milling system. Correspondingly, the vibration base frequency will be superimposed to f_{TPF} to form chatter frequencies. It can be seen that due to the multi-order properties of f_{TPF}, the chatter frequencies also present multi-order properties. The chatter frequencies can be expressed as shown in Eq. (3).

$$f_{MCF} = |f_C \pm f_{TPF}|(\text{Hz}) \tag{3}$$

Note that the frequency components f_{TPF}, f_{MCF}, and f_C are all positive values. Eq. (3) can be transformed as $f_C = |f_{MCF} - f_{TPF}|$(Hz). It can be observed that the difference between tooth pass frequency and chatter frequency is a constant value f_C. The vibration base frequency is a direct and inherent feature for chatter. Thus, the difference is introduced as a feature in chatter identification.

Figure 5a, b shows the cutting force signal and its spectrums of one of the preliminary chatter experiments, respectively. The detailed cutting parameters are as follow: f_z is 0.15 mm/tooth, a_e is 0.5 mm, a_p is 8 mm, and n is 6000 rpm. Thus, f_{SRF} and f_{TPF} of the experiment are $100m$ Hz and $200m$ Hz ($m = 1, 2, \ldots$), respectively, and correspondingly marks as blue triangles and red rectangles, respectively. The yellow circles are marked as the identified maximum frequency components f_{IMF} except the f_{SRF} in the interval of two adjacent f_{TPF}. It can be seen that the differences between the f_{IMF} and the f_{TPF} are a fairly stable frequency 62 Hz. For example, 2200–2138 = 62 Hz (2200 = 200 × 11) and 3400–3338 = 62 Hz (3400 = 200 × 17). That is to say, $f_{IMF} = f_{TPF}$-62 Hz which accord with Eq. (3). The milling condition can be identified as chatter. In such case, f_{IMF} can be regarded as the chatter frequencies f_{MCF}. The fairly stable frequency component 62 Hz is the vibration base frequency f_C. Thus, the core of chatter identification is to search the maximum frequency component and calculate if a steady vibration base frequency exists. The following will give a detailed description of the proposed algorithm.

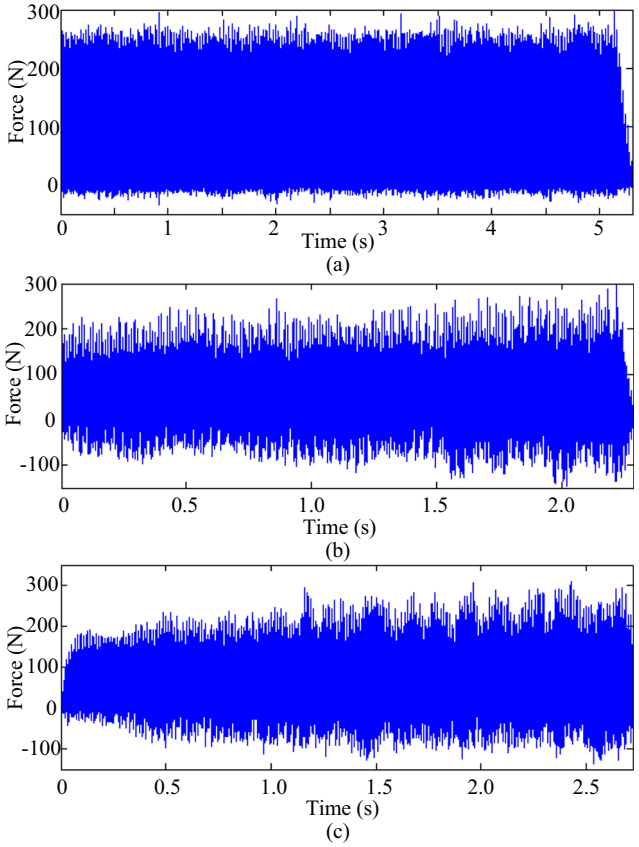

Fig. 9 Cutting force signal of **a** test 1, **b** test 3, and **c** test 5

3.2 Frequency-domain search algorithm

Step 1. Determine the multiple of the initial search frequency k_b.

Figure 5c shows the schematic diagram of the FDS algorithm. Here, the spindle speed is n, the number of teeth is N_t. k is a temporary variable whose initial value equals to 1. The searching range for the FDS algorithm is defined as $[f^a_{cfr}, f^b_{cfr}]$, which will be determined in Sect. 3.3. Gradually

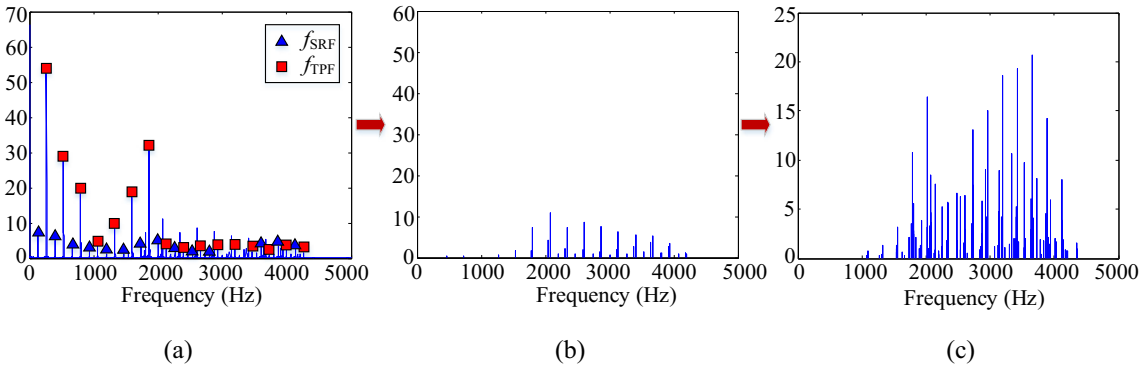

Fig. 8 Analysis of frequency range for chatter. **a** Original spectrum of cutting force (test 7). **b** Spectrum where f_{SRF} and f_{TPF} are filtered (test 7). **c** The superposition of the spectrums of all the test where f_{SRF} and f_{TPF} are filtered

increase k and judge whether $knN_t/60 \geq f_{\mathrm{cfr}}^{a}$. If meet the condition, $k_{\mathrm{b}} = k$.

Step 2. Divide the interval for frequency-domain search.

Define the open interval $((k_{\mathrm{b}}+i-1)f_{\mathrm{TPF}}, (k_{\mathrm{b}}+i)f_{\mathrm{TPF}})$ as the searching interval, where $i = 1, 2, \cdots$ is the increment of frequency doubling. It can be seen that any two adjacent f_{TPF} is an interval for the frequency domain search.

Step 3. Search the maximum frequency component.

Search the maximum frequency component in the interval $((k_{\mathrm{b}}+i-1)f_{\mathrm{TPF}}, (k_{\mathrm{b}}+i)f_{\mathrm{TPF}})$. Mark the searched maximum frequency components as $f_{\mathrm{IMF}}(i)$. Calculate the difference between $f_{\mathrm{IMF}}(i)$ and f_{TPF}, namely $f_{\mathrm{d}}(i) = (k_{\mathrm{b}}+i-1)f_{\mathrm{TPF}} - f_{\mathrm{IMF}}(i)$. If $(k_{\mathrm{b}}+i-1)f_{\mathrm{TPF}} \geq f_{\mathrm{cfr}}^{b}$, stop the search.

Step 4. Judge the vibration base frequency.

If there is a steady vibration base frequency in the above calculation, the milling condition is labeled as chatter. In such case, the identified maximum frequency components are the chatter frequencies. Otherwise, the milling condition is

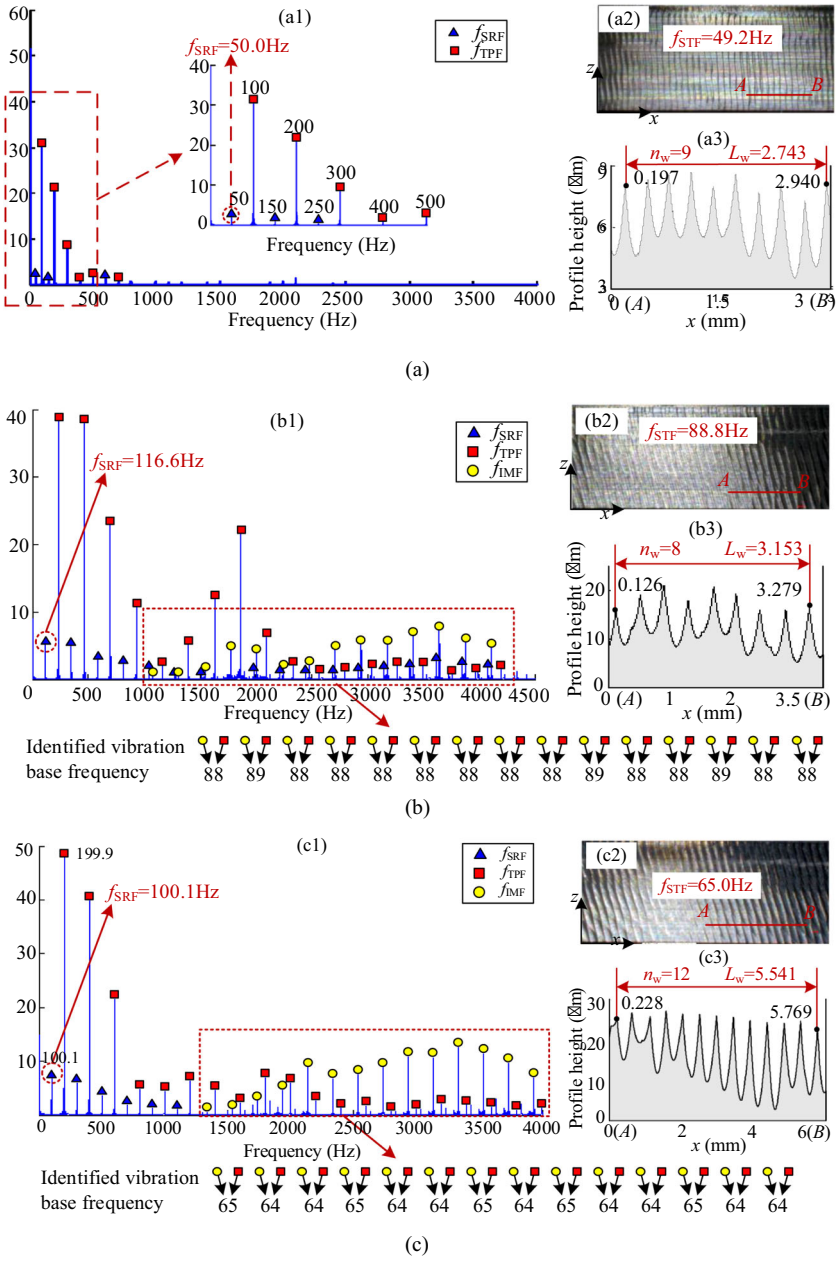

Fig. 10 Chatter analysis of **a** test 1 (n = 3000 rpm), **b** test 3 (n = 7000 rpm), and **c** test 5 (n = 6000 rpm) (1, Spectral analysis of the cutting force signal. 2, Surface topography measured by ultra-depth of field microscope. 3, Surface profile)

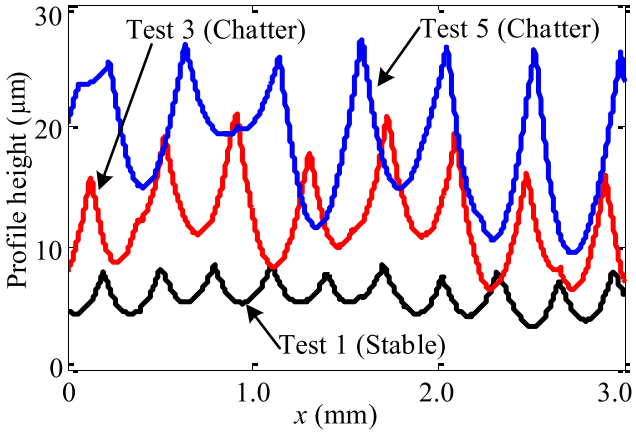

Fig. 11 Comparison of surface profiles of **a** test 1 (n = 3000 rpm), **b** test 3 (n = 7000 rpm), and **c** test 5 (n = 6000 rpm)

labeled as stable. Figure 6 shows the flowchart of the chatter identification based on the proposed FDS algorithm.

3.3 Determination of the searching range of the proposed algorithm

In order to improve the searching accuracy and the efficiency of the proposed algorithm, this section will discuss the selection of the appropriate direction of cutting force signal and the searching range for the proposed algorithm. As well known, milling action mainly concentrates on low-frequency range, while the chatter action mainly focuses on the high-frequency range. Figure 7a, b shows the cutting force and its spectrum in x and y directions, respectively. Obviously, the frequency components in the high-frequency range in the x direction are more plentiful and remarkable than in the y direction. Thus, the cutting force signal in the x direction is selected for the proposed algorithm.

As described above, the spectrum of the cutting force signal mainly comprises f_{SRF} and f_{TPF}. The chatter frequencies exist in the occurrence of chatter milling. Figure 8a, b shows the original spectrum and the spectrum where f_{SRF} and f_{TPF} have been filtered. Figure 8c shows the superposition of frequency components of all the proposed chatter experiments where the f_{SRF} and f_{TPF} are filtered. It can be seen that there are no prominent frequency components within the range of 0–1000 Hz. The reason is that the f_{SRF} and f_{TPF} representing the cutting action have been removed accordingly. The remainder frequency components mainly concentrate in the range of 1000–4500 Hz. That is to say, the chatter frequency components are prone to appear in this range. Thus, the cutting force signal in x direction and the searching range of 1000–4500 Hz are determined for the proposed algorithm to accurately and efficiently identify the milling chatter. Correspondingly, f_{cfr}^{a} = 1000 Hz and f_{cfr}^{b} = 4500 Hz.

4 Validation

4.1 Validation and analysis of the effectiveness of the proposed algorithm using force signal

In this section, tests 1, 3, and 5 are selected to make a detailed analysis. Figure 9a shows the cutting force signal of these three experiments where the milling conditions are stable, chatter, and chatter, respectively. Obviously, the variation of the amplitude of cutting force under stable milling is basically stable. Figure 9c shows a typical cutting force signal of milling chatter where there is an obvious increasing trend on its amplitude. However, the increasing trend shown in Fig. 9b is not obvious, although the milling condition of test 3 belongs to chatter. In such case, it is difficult to distinguish the milling condition just according to the variation of cutting force, especially the occurrence of the slight chatter.

Figure 10 (a1) shows the spectral analysis of test 1. It can be seen that the spectrum of test 1 mainly comprises f_{SRF} and f_{TPF}. There are no new frequency components within the entire frequency range. Correspondingly, a stable vibration base frequency cannot be identified based on the proposed algorithm. Thus, the milling condition is identified as stable, which accords with the experimental result. Figure 10 (b1) shows the spectral analysis of test 2. The yellow circle represents the identified maximum frequency components (f_{IMF}) between two adjacent f_{TPF}. Obviously, a new frequency component appears in test 2. Further, the identified vibration base frequency is given in Fig. 10b. It can be seen that the vibration base frequency is fairly stable which is located in the set of {88, 89}. Thus, the milling condition is identified as chatter, which accords with the experimental result. The same analysis can be found in Fig. 10c. The identified vibration base

Table 4 Comparison of the identified and experimental milling conditions when using force signal

	Test 1	Test 2	Test 3	Test 4	Test 5	Test 6	Test 7
f_{SRF} (Hz)	50	133.4	116.6	133.4	100	116.6	133.4
f_C (Hz)	–	{68, 69}	{88, 89}	{65, 66}	{64, 65}	{75, 76}	{61, 62}
f_{STF} (Hz)	50	68.4	88.8	65.7	65.0	75.4	61.6
Identified	Stable	Chatter	Chatter	Chatter	Chatter	Chatter	Chatter
Experimental	Stable	Chatter	Chatter	Chatter	Chatter	Chatter	Chatter

frequency of test 3 locates in the set of {64, 65}. The milling condition of test 3 is thus identified as chatter which also accords with the experimental result. Based on the above analysis, it can be seen that the proposed algorithm can accurately identify stable and chatter condition during the milling process. Meanwhile, the extracted feature, the vibration base frequency does not need to set a threshold to distinguish the chatter and stable machining.

Figure 11 shows the comparison of the surface profiles giving in Fig. 10 (a3–c3). It can be seen that the peaks and valleys of the surface profile under chatter machining are significantly greater than those under the stable machining. This accords with the characteristics of chatter machining where the dramatical relative vibration between the tool and workpiece will deteriorate the surface quality as well as the variation of the large amplitude of the surface profiles [15]. Further, the variation of the peaks and valleys of the surface profiles under chatter machining also reflects the severity of the chatter. The amplitude of surface profiles of test 5 is obviously greater than test 3. That is to say, the chatter severity of test 5 is large than test 3 which can be reflected in the comparison of Fig. 10 (b2 and c2).

In addition, it can be seen from Fig. 10 (a2, b2, and c2) that the corrugated appearance exists on the machined workpiece surface. Here, a surface topography frequency (f_{STF}) is introduced to depict the variation of the existing corrugated appearances. f_{STF} is defined as the number of corrugated appearance per unit feed length. The calculation of f_{STF} is given in Eq. (4).

$$f_{STF} = \frac{n_w \cdot n \cdot f_z \cdot N_t}{60 \times L_w} \tag{4}$$

where L_w is the measured length of surface profile, n_w represents the number of the corrugations in the scope of L_w. As shown in Fig. 10 (a2, b2, and c2), AB is the selected surface profile for calculation. The following will give a discussion on the relationship between f_C and f_{STF}.

Based on Eq. (4), f_{STF} of tests 1, 3, and 5 are calculated as 50, 88.8, and 65.0 Hz, respectively. The identified f_C (tests 3 and 5) accords with the experimental result. In addition, it is found that in the stable milling (test 1), f_{STF} just equals to f_{SRF}. It proves that the corrugated appearance under stable milling is mainly due to the cutting action. In the chatter milling (tests 3 and 5), the f_{STF} just equals to the new appeared base frequency. That is to say, the corrugated appearance is mainly due to the chatter action. Meanwhile, it can be concluded that the proposed algorithm can accurately identify the vibration base frequency of chatter.

Table 4 gives a comparison of the identified and experimental conditions. The stable vibration base frequency is identified in all the chatter milling experiments. Further, all

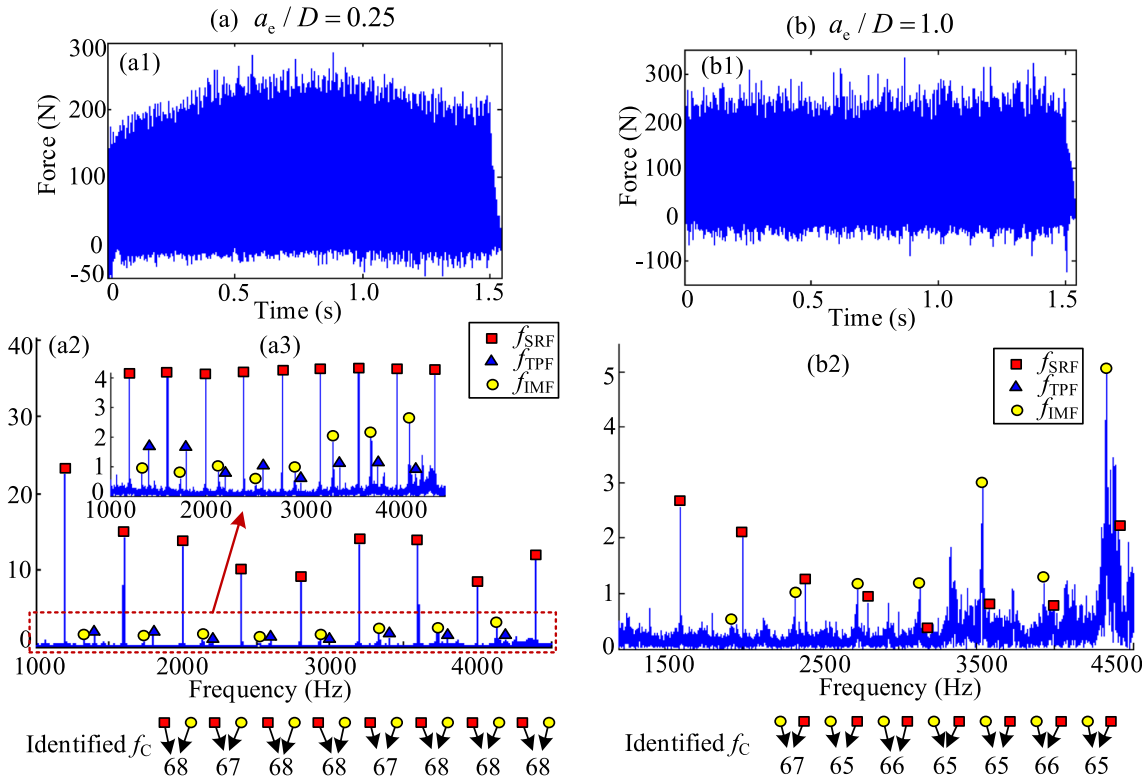

Fig. 12 Chatter analysis of **a** a_e/D = 0.25 (a1, cutting force signal; a2 and a3, spectral analysis; a_e = 1.5 mm, n = 6000 rpm, a_p = 1 mm, f = 0.15 mm/tooth); **b** a_e/D = 1.0 (b1, cutting force signal; b2, spectral analysis; a_e = 6 mm, n = 6000 rpm, a_p = 1 mm, f = 0.15 mm/tooth)

the identified f_C are almost exactly equal to its f_{STF}. Based on the proposed FDS algorithm, the identified milling conditions of tests 2–7 belong to chatter, which accords with the experimental results. It proves that the proposed algorithm is effective in milling chatter identification.

4.2 Validation of the effectiveness of the FDS algorithm on different radial immersion ratios

The above section validates the effectiveness of the proposed algorithm where the spindle speed and axial depth of cut a_p is changing, and the radial depth of cut a_e is fixed. In such case, the radial immersion ratio $a_e/D = 0.083$. That is to say, the proposed algorithm is effective on a low radial immersion ratio. To further test the robustness of the proposed algorithm on different radial immersion ratios, two experiments with $a_e/D = 0.25$ and $a_e/D = 1.0$ are carried out, and its experimental conditions both belong to chatter. $a_e/D = 1.0$ represents the full slotting. For the first experiment with $a_e/D = 0.25$, a_e = 1.5 mm, $n = 6000$ rpm, $a_p = 1$ mm, and $f = 0.15$ mm/tooth. For the second experiment with $a_e/D = 1.0$, $a_e = 6$ mm, $n = 6000$ rpm, $a_p = 1$ mm, and $f = 0.15$ mm/tooth. Figure 12a, b shows the spectral analysis of experiments with $a_e/D = 0.25$ and $a_e/D = 1.0$, respectively. It can be seen that both fairly stable f_C can be identified based on the FDS algorithm. Thus, the milling conditions of the two experiments are identified as chatter, which accord with the experimental results. It proves that the proposed algorithm is also effective on the various radial depth of cut ranging from very low radial immersion ratio to full slotting.

4.3 Validation of the effectiveness of the FDS algorithm when using a small amount of signal data

This section will validate the effectiveness of the proposed algorithm when using a small amount of signal data. Figure 13a shows the cutting force of test 5. Figure 13 (b1 and b2) shows the cutting force signal in the period of 0.3 s and its spectrum. The machining condition cannot be directly judged only based on the variation of the small part of cutting force signals. Meanwhile, it can be seen that its spectrum mainly focuses on low-frequency range. The amplitude of spectrum in the high-frequency range is relatively very low, which means that the vibration action is not significant. Figure 13 (b3) shows the spectrum of 1000–2200 Hz. It is found that only the f_{SRF} and f_{TPF} appear. The chatter frequency is not identified in this range. Figure 13 (b4) shows the spectrum of 2200–2900 Hz. It can be seen that a steady base frequency in set of {63, 64} Hz is identified which proves the appearance of the chatter. The yellow circles are the corresponding identified chatter frequencies. The amplitude of chatter frequencies is very low, which means that the chatter action in this period of time is very slight. It can be concluded

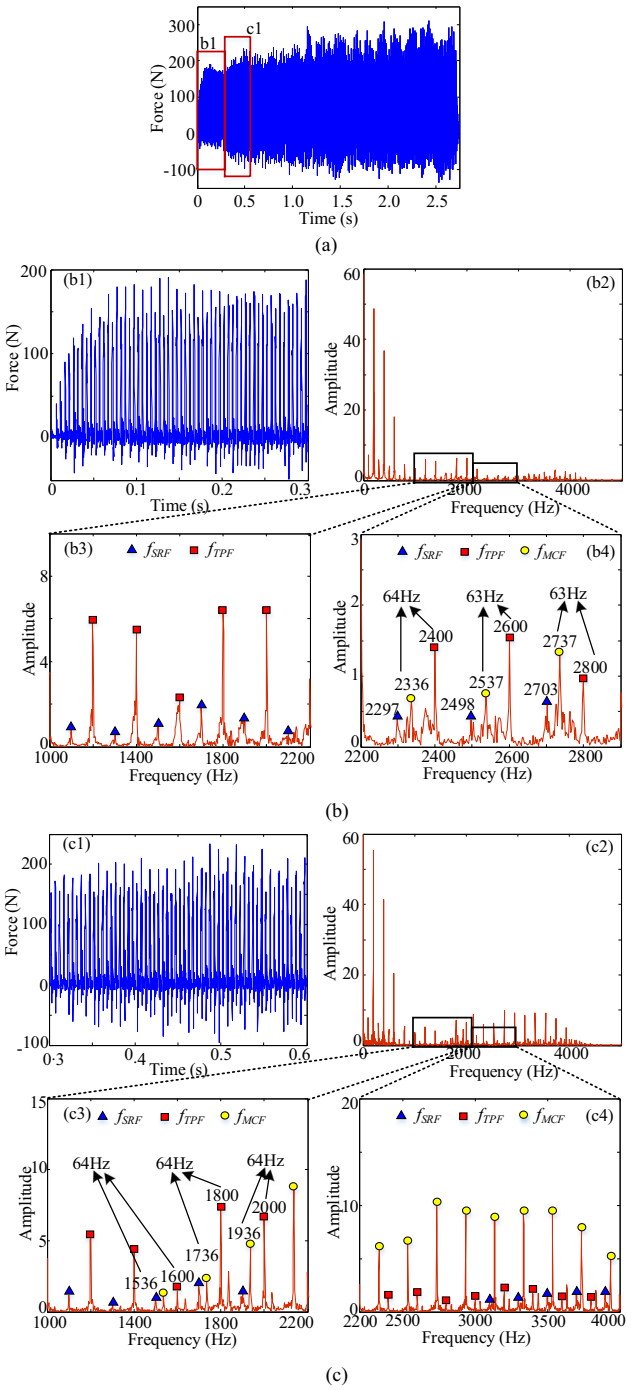

Fig. 13 Analysis and validation of FDS algorithm when using a small amount of signal data. **a** The original cutting force signal. **b** Spectral analysis of the cutting force signal of part (b1). **c** Spectral analysis of the cutting force signal of part (c1)

that the proposed algorithm can accurately identify the chatter, even the slight chatter in the initial stage of machining can be effectively identified.

Figure 13 (c1 and c2) shows the cutting force signal in the period from 0.3 to 0.6 s and its spectrum. Compared with Fig. 13 (b2), it is found that the amplitude of the spectrum in

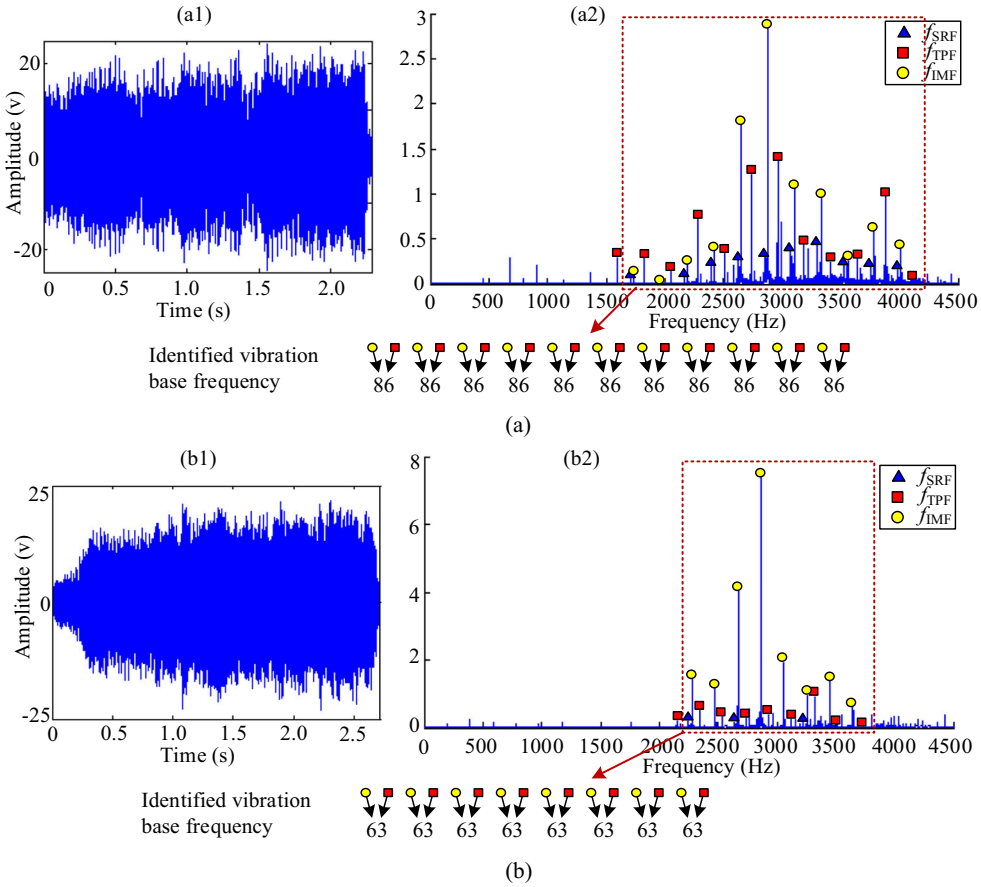

Fig. 14 Chatter analysis of vibration signal. **a** Test 3 (n = 7000 rpm). **b** Test 5 (n = 6000 rpm) (a1 and b1 represent the vibration signal; a2 and b2 represent the spectrum of the vibration signal)

the high-frequency range shown in Fig. 13 (c2) significantly increases. That is to say, the vibration action in this stage is enhanced. A steady vibration base frequency is identified in the range of 1000–2200 Hz, as shown in Fig. 13 (c3). This is mainly due to the enhancement of the chatter action. This point can also be reflected in Fig. 13 (c4), where the amplitude of chatter frequency dramatically increases. The above analysis proves that the proposed algorithm is effective in chatter identification when using a small amount of signal data.

4.4 Validation of the effectiveness of the FDS algorithm when using vibration signal

This section will validate the effectiveness of the proposed algorithm when using vibration signals. Figure 14 (a1 and a2) represents the vibration signal and its spectral analysis of test 3. It can be seen that the spectrum of the vibration signal mainly focuses on the high-frequency range. Further, a stable f_C 86 Hz can be identified based on the FDS algorithm. The identified vibration base frequency accords with the f_{STF} of test 3. That is to say, the identified milling condition is chatter, which accords with the experimental result. Figure 14 (b1 and b2) represents the vibration signal and its spectral analysis of test 5. It can be seen that the identified f_C is 63 Hz which accords with the f_{STF} of test 5. The milling condition of test 5 is identified as chatter which accords with the experimental result. Table 5 gives the comparison of the identified and experimental conditions when using vibration signal. All the identified milling conditions accord with the experimental results. The results demonstrate the effectiveness of the proposed algorithm in milling chatter identification when using the vibration signal.

Table 5 Comparison of the identified and experimental milling conditions when using vibration signal

	Test 1	Test 2	Test 3	Test 4	Test 5	Test 6	Test 7
f_C (Hz)	–	{66, 67}	86	{64, 65}	63	{73, 74}	60
f_{STF} (Hz)	50	68.4	88.8	65.7	65.0	75.4	61.6
Identified	Stable	Chatter	Chatter	Chatter	Chatter	Chatter	Chatter
Experimental	Stable	Chatter	Chatter	Chatter	Chatter	Chatter	Chatter

5 Discussions

5.1 The relationship among the natural frequency, cutting parameters, and chatter frequency

Note that the chatter is closely related to the characteristics of the spindle-tool system. Meanwhile, the occurrence of the chatter is also affected by the cutting conditions. Thus, the analysis of the relationship among the chatter frequency, the natural frequency of the spindle-tool system, and the cutting parameters are of significance. Figure 15a shows the variation of chatter frequency of the six sets of chatter tests. Note that the chatter frequencies are normalized in which each chatter frequency is divided by the maximum chatter frequency. Zone A represents one of the dominant chatter frequencies which locates within the range of 1900–2200 Hz. Figure 15b shows the measured natural frequency of the spindle-tool system in x and y direction, respectively as described in Sect. 2.1. Dominant chatter frequencies are found around the second-order natural frequency of the spindle-tool system but do not exactly equal to the second-order natural frequency. Meanwhile, it is found that there are no dominant chatter frequencies around the first-order natural frequency. That is to say, the dominant chatter frequencies appear around the certain order of the natural frequency of the system but not each order of natural frequency.

Figure 16 shows the variation of the vibration base frequency with spindle speed and axial depth of cut. It can be seen that the vibration base frequency varies with the change of cutting parameters, but there is no obvious law. For example, the cutting parameters of tests 4 and 5 are different, but the vibration base frequency is the same. For tests 2, 4, and 7, the spindle speeds are all 8000 rpm and the axial depth of cut varies from 4 to 6 mm. That is to say, they have the same

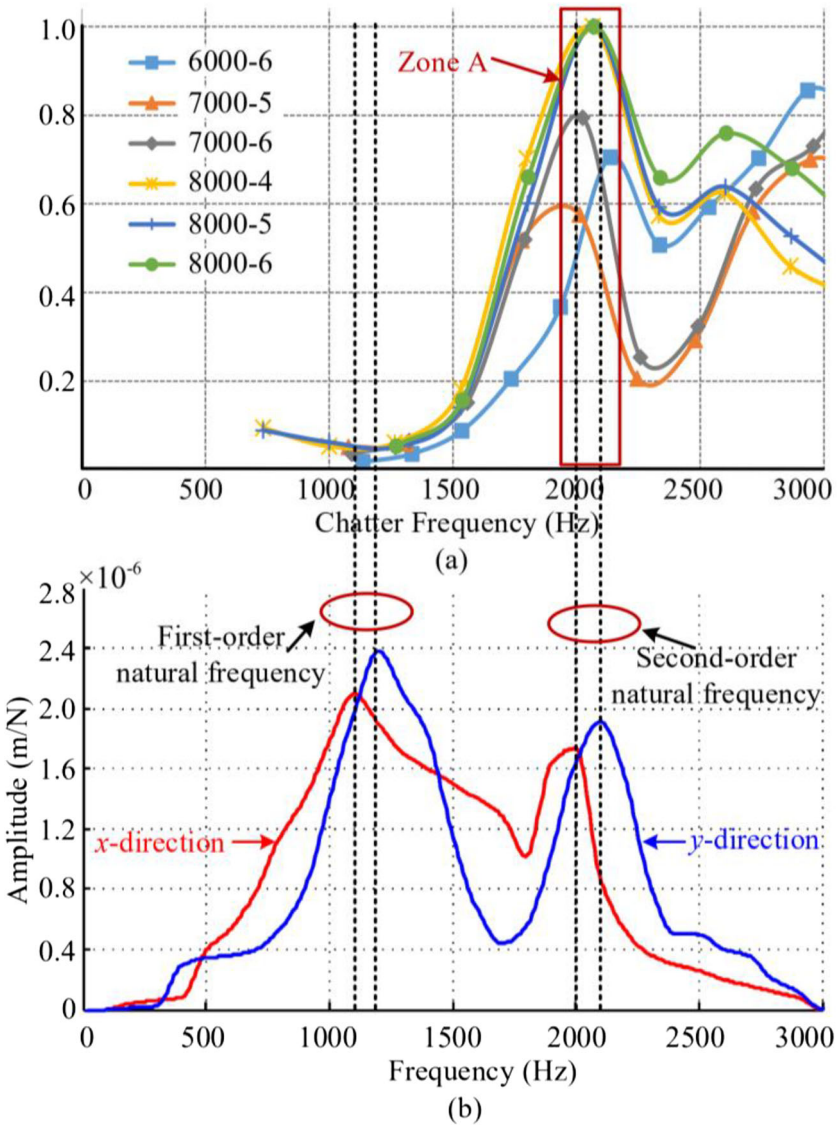

Fig. 15 The relationship between chatter frequencies and the natural frequency of the spindle-tool system. **a** The variation of the chatter frequencies. **b** Natural frequency of the spindle-tool system including first- and second-order natural frequencies

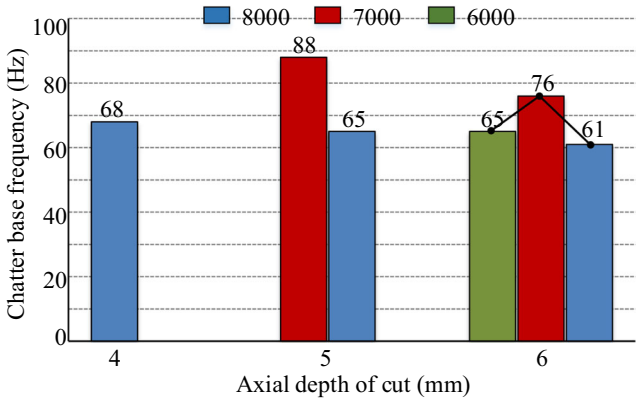

Fig. 16 Variation of vibration base frequency with cutting parameters

spindle rotation frequency. However, the vibration base frequency of these three tests varies from 68 to 61 Hz. In such case, the chatter frequencies of these three tests are certainly different according to Eq. (3). That is to say, cutting parameters will affect the chatter frequencies. Based on the above analysis, it can be concluded that the chatter frequencies are determined by the combination of the natural frequency of the spindle-tool system and the cutting parameters.

6 Conclusions

The main contribution of the paper is that a novel FDS algorithm is proposed to identify the milling chatter whether using the cutting force signal or the vibration signal. Compared with the existing methods on the chatter identification, the proposed algorithm has three main characteristics. The first is that the FDS algorithm does not need many complicated signal processing algorithms before feature extraction which ensures the simplicity of the method. The second is that an inherent feature of chatter named vibration base frequency is directly extracted to identify the chatter and stable condition. The extracted feature does not need to set threshold according to different machining conditions. The third is that only a small amount of signal data is needed for identification which guarantees the timeliness of the chatter identification.

Hammer test and milling experiments with various cutting parameters are carried out, and both force signal and vibration signal in the experiments are utilized to validate the effectiveness of the proposed algorithm. The results prove that the FDS algorithm can accurately identify the milling chatter and correspondingly identify the multiple chatter frequencies, and even the slight chatter in the initial machining stage can be identified. Further analysis shows that the dominant chatter frequencies will appear around the certain order of the natural frequency of the spindle-tool system but do not exactly equal to the natural frequency. The chatter frequencies are determined by the combination of the natural characteristics of the system and the cutting condition. The proposed algorithm is expected to be a viable tool in chatter identification in the industry.

Acknowledgments This project is supported by the Natural Science Foundation of Tianjin (No. 18JCQNJC75600), National Natural Science Foundation of China (No. 51705362), and Science & Technology Development Fund of Tianjin Education Commission for Higher Education (No. 2017KJ081).

References

1. Yang K, Wang GF, Dong Y, Zhang QB, Sang LL (2019) Early chatter identification based on an optimized variational mode decomposition. Mech Syst Signal Pr 115:238–254. https://doi.org/10.1016/j.ymssp.2018.05.052
2. Aslan D, Altintas Y (2018) On-line chatter detection in milling using drive motor current commands extracted from CNC. Int J Mach Tool Manu 132:64–80. https://doi.org/10.1016/j.ijmachtools.2018.04.007
3. Catania G, Mancinelli N (2011) Theoretical-experimental modeling of milling machines for the prediction of chatter vibration. Int J Mach Tool Manu 51:339–348. https://doi.org/10.1016/j.ijmachtools.2018.04.007
4. Kayhan M, Budak E (2009) An experimental investigation of chatter effects on tool life. P I Mech Eng B-J Eng 223(11):1455–1463. https://doi.org/10.1243/09544054JEM1506
5. Li ZQ, Wang ZK, Shi XF (2017) Fast prediction of chatter stability lobe diagram for milling process using frequency response function or modal parameters. Int J Adv Manuf Technol 89:2603–2612. https://doi.org/10.1007/s00170-016-9959-4
6. Grossi N, Montevecchi F, Sallese L, Scippa A, Campatelli G (2017) Chatter stability prediction for high-speed milling through a novel experimental-analytical approach. Int J Adv Manuf Technol 89:2587–2601. https://doi.org/10.1007/s00170-016-9832-5
7. Graham E, Mehrpouya M, Park SS (2013) Robust prediction of chatter stability in milling based on the analytical chatter stability. J Manuf Process 15:508–517. https://doi.org/10.1016/j.jmapro.2013.08.005
8. Altintas Y, Budak E (1995) Analytical prediction of stability lobes in milling. CIRP Ann-Manuf Techn 44:357–362. https://doi.org/10.1016/S0007-8506(07)62342-7
9. Najafi B, Hakim H (1992) A comparative study of non-parametric spectral estimators for application in machining vibration analysis. Mech Syst Signal Pr 6:551–574. https://doi.org/10.1016/0888-3270(92)90049-O
10. Lamraoui M, Thomas M, El Badaoui M, Girardin F (2014) Indicators for monitoring chatter in milling based on instantaneous angular speeds. Mech Syst Signal Pr 44:72–85. https://doi.org/10.1016/j.ymssp.2013.05.002
11. Suh CS, Khurjekar PP, Yang B (2002) Characterisation and identification of dynamic instability in milling operation. Mech Syst Signal Pr 16(5):853–872. https://doi.org/10.1006/mssp.2002.1497
12. Feng JL, Sun ZL, Jiang ZH, Yang L (2016) Identification of chatter in milling of Ti-6Al-4V titanium alloy thin-walled workpieces based on cutting force signals and surface topography. Int J Adv Manuf Technol 82:1909–1920. https://doi.org/10.1007/s00170-015-7509-0
13. Kuljanic E, Sortino M, Totis G (2008) Multisensor approaches for chatter detection in milling. J Sound Vib 312:672–693. https://doi.org/10.1016/j.jsv.2007.11.006
14. Niu JC, Ning GC, Shen YJ, Yang SP (2019) Detection and identification of cutting chatter based on improved variational nonlinear

chirp mode decomposition. Int J Adv Manuf Technol 104:2567–2578. https://doi.org/10.1007/s00170-019-04035-z
15. Gao J, Song QH, Liu ZQ (2018) Chatter detection and stability region acquisition in thin-walled workpiece milling based on CMWT. Int J Adv Manuf Technol 98:699–713. https://doi.org/10.1007/s00170-018-2306-1
16. Ye J, Feng PF, Xu C, Ma Y, Huang SG (2018) A novel approach for chatter online monitoring using coefficient of variation in machining process. Int J Adv Manuf Technol 96:287–297. https://doi.org/10.1007/s00170-017-1544-y
17. Ji YJ, Wang XB, Liu ZB, Yan ZH, Jiao L, Wang DQ, Wang JQ (2017) EEMD-based online milling chatter detection by fractal dimension and power spectral entropy. Int J Adv Manuf Technol 92:1185–1200. https://doi.org/10.1007/s00170-017-0183-7
18. Fu Y, Zhang Y, Zhou H, Li DQ, Liu HQ, Qiao HY, Wang XQ (2016) Timely online chatter detection in end milling process. Mech Syst Signal Pr 75:668–688. https://doi.org/10.1016/j.ymssp.2016.01.003
19. Cao HR, Zhou K, Chen XF, Zhang XW (2017) Early chatter detection in end milling based on multi-feature fusion and 3σ criterion. Int J Adv Manuf Technol 92:4387–4397. https://doi.org/10.1007/s00170-017-0476-x
20. Li K, He SP, Luo B, Li B, Liu HQ, Mao XY (2019) Online chatter detection in milling process based on VMD and multiscale entropy. Int J Adv Manuf Technol 105:5009–5022. https://doi.org/10.1007/s00170-019-04478-4
21. Chen GS, Zheng QZ (2018) Online chatter detection of the end milling based on wavelet packet transform and support vector machine recursive feature elimination. Int J Adv Manuf Technol 95:775–784. https://doi.org/10.1007/s00170-017-1242-9
22. Cao HR, Lei YG, He ZJ (2013) Chatter identification in end milling process using wavelet packets and Hilbert-Huang transform. Int J Mach Tool Manu 69:11–19. https://doi.org/10.1016/j.ijmachtools.2013.02.007
23. Choi T, Shin YC (2003) Online chatter detection using wavelet-based parameter estimation. J Manuf Sci E-T ASME 125(1):21–28. https://doi.org/10.1115/1.1531113
24. Al-Regib E, Ni J (2010) Chatter detection in machining using nonlinear energy operator. J Dyn Syst-T ASME 132:034502(1-4). https://doi.org/10.1115/1.4001331
25. Caliskan H, Kilic ZM, Altintas Y (2018) Online energy-based milling chatter detection. J Manuf Sci E-T ASME 140:111012 (1-12). https://doi.org/10.1115/1.4040617
26. Liu HB, Bo QL, Zhang H, Wang YQ (2018) Analysis of Q-factor's identification ability for thin-walled part flank and mirror milling chatter. Int J Adv Manuf Technol 99:1673–1686. https://doi.org/10.1007/s00170-018-2580-y
27. Wang GF, Dong HY, Guo YJ, Ke YL (2018) Early chatter identification of robotic boring process using measured force of dynamometer. Int J Adv Manuf Technol 94:1243–1252. https://doi.org/10.1007/s00170-017-0941-6
28. Zhang Z, Li HG, Meng G, Tu XT, Cheng CM (2016) Chatter detection in milling process based on the energy entropy of VMD and WPD. Int J Mach Tool Manu 108:106–112. https://doi.org/10.1016/j.ijmachtools.2016.06.002
29. Berger B, Belai C, Anand D (2003) Chatter identification with mutual information. J Sound Vib 267(1):178–186. https://doi.org/10.1016/S0022-460X(03)00067
30. Schmitz TL (2003) Chatter recognition by a statistical evaluation of the synchronously sampled audio signal. J Sound Vib 262(3):721–730. https://doi.org/10.1016/S0022-460X(03)00119-6
31. Rusinek R, Lajmert P, Kecik K, Kruszynski B, Warminski J (2015) Chatter identification methods on the basis of time series measured during titanium superalloy milling. Int J Mech Sci 99:196–207. https://doi.org/10.1016/j.ijmecsci.2015.05.013
32. Shao YM, Deng X, Yuan YL, Mechefske CK, Chen ZG (2014) Characteristic recognition of chatter mark vibration in a rolling mill based on the non-dimensional parameters of the vibration signal. J Mech Sci Technol 28(6):2075–2080. https://doi.org/10.1007/s12206-014-0106-6
33. Ma L, Melkote SN, Castle JB (2013) A model based computationally efficient method for on-line detection of chatter in milling. J Manuf Sci E-T ASME 135(3):1–11. https://doi.org/10.1115/MSEC2013-1031
34. van Dijk NJM, Doppenberg EJJ, Faassen RPH, van de Wouw N, Oosterling JAJ, Nijmeijer H (2010) Automatic in-process chatter avoidance in the high-speed milling process. J Dyn Syst-T ASME 132(3):333–342. https://doi.org/10.1115/1.4000821
35. Wan SK, Li XH, Chen W, Hong J (2018) Investigation on milling chatter identification at early stage with variance ratio and Hilbert-Huang transform. Int J Adv Manuf Technol 95:3563–3573. https://doi.org/10.1007/s00170-017-1410-y
36. Insperger T, Stépán G, Bayly PV, Mann BP (2003) Multiple chatter frequencies in milling processes. J Sound Vib 262:333–345. https://doi.org/10.1016/S0022-460X(02)01131-8
37. Dombovari Z, Iglesias A, Zatarain M, Insperger T (2011) Prediction of multiple dominant chatter frequencies in milling process. Int J Mach Tool Manu 51:457–464. https://doi.org/10.1016/j.ijmachtools.2011.02.002
38. Wang GF, Peng DB, Qin XD, Cui YH (2012) An improved dynamic milling force coefficients identification method considering edge force. J Mech Sci Technol 26(5):1585–1590. https://doi.org/10.1007/s12206-012-0306-x
39. Ding Y, Zhu LM, Zhang XJ, Ding H (2010) A full-discretization method for prediction of milling stability. Int J Mach Tool Manu 50:502–509. https://doi.org/10.1016/j.ijmachtools.2010.01.003